REPORT DOCUMENTATION PAGE

Form Approved
OMB NO. 0704-0188

1. AGENCY USE ONLY (Leave Blank)	2. REPORT DATE	3. REPORT TYPE AND DATES COVERED
	9/15/97	Final Report - 5/14/93 - 5/13/96

4. TITLE AND SUBTITLE

Photonic Band Structure for Optical Inter-Connect Arrays & Logic Functions

5. FUNDING NUMBERS

DAAH04-93-G-0227

6. AUTHOR(S)

Eli Yablonovitch

7. PERFORMING ORGANIZATION NAME(S) AND ADDRESS(ES)

University of California, Los Angeles
Electrical Engineering Dept.
Los Angeles, CA 90095-1594

8. PERFORMING ORGANIZATION REPORT NUMBER

KD3XFinal

9. SPONSORING / MONITORING AGENCY NAME(S) AND ADDRESS(ES)

U. S. Army Research Office
P.O. Box 12211
Research Triangle Park, NC 27709-2211

10. SPONSORING / MONITORING AGENCY REPORT NUMBER

ARO 31237.11-PH

11. SUPPLEMENTARY NOTES

The views, opinions and/or findings contained in this report are those of the author(s) and should not be construed as an official Department of the Army position, policy or decision, unless so designated by the documentation.

12 a. DISTRIBUTION / AVAILABILITY STATEMENT

Approved for public release; distribution unlimited

19971204 090

13. ABSTRACT (Maximum 200 words)

We have investigated the electromagnetic properties of a two dimensional photonic crystal array of vertical cavities for use in nonlinear optical image processing. We have determined the two dimensional photonic band structure of the array, and we discuss how it is influenced by the degree of interaction between cavities. We have studied the properties of defects in the 2-D lattice, and have shown that neighboring cavities will interact through their overlapping wave functions. This interaction can be used to produce nearest neighbor nonlinear Boolean functions such as AND, OR, and XOR which are useful for optical image processing. We demonstrate the use of 2-D photonic band gap structures for image processing by removing noise from a sample image, employing a nearest neighbor AND function.

14. SUBJECT TERMS

Photonic band-gap structures, Photonic Crystals, Optical Image Processing
Nonlinear Image Processing

15. NUMBER OF PAGES

16. PRICE CODE

17. SECURITY CLASSIFICATION OR REPORT	18. SECURITY CLASSIFICATION ON THIS PAGE	19. SECURITY CLASSIFICATION OF ABSTRACT	20. LIMITATION OF ABSTRACT
UNCLASSIFIED	UNCLASSIFIED	UNCLASSIFIED	UL

NSN 7540-01-280-5500

Standard Form 298 (Rev.2-89)
Prescribed by ANSI Std. 239-18
298-102

Photonic Band Structure for Optical Inter-Connect Arrays & Logic Functions

Final Progress Report

Eli Yablonovitch

Period covered : 5/14/93 - 5/13/96

U.S. Army Research Office

Award Number: DAAH04-93-G-0227

Proposal Number: 31237-PH

University of California, Los Angeles

Final Report
Photonic Band Structure for Optical Inter-Connect Arrays & Logic Functions
Award Number: DAAH04-93-G-0227
Proposal Number: 31237-PH

1. Statement of problem studied:

We studied the prospects for making 2-d arrays of fully confined 3-d photonic crystals, and 2-d Fabry-Perot Spatial Light Modulator Arrays, (FPSLMA's), where the coupling between pixels creates a 2-d superlattice photonic band structure at a correspondingly longer length scale. The interaction between pixels, which produces the 2-d electromagnetic band structure, also allows parallel Boolean logic functions between them, as well as nonlinear image processing. We engineered a 2-d band structure where smart pixels arise purely from electromagnetic interactions, without requiring conventional Silicon logic.

2. Summary of the most important results:

For the 3-d photonic crystals at optical wavelengths, the important result was the creation by nano-lithography of a PBG material which was forbidden between 1.1microns and 1.5microns wavelength. However the rejection ratio was only 87% at best, and the 3-d structures will require more work. For the Boolean logic functions, and nonlinear image processing we created 2-d vertical cavity arrays, at microwave-lengths. This array successfully performed nonlinear noise removal from a 2-d image. The pre-print of this work is attached.

3. Publications and technical reports published

Yablonovitch, E. "Photonic Crystals," J. Modern Optics, Vol. 41(2), pp. 173-194, 1994.

Yablonovitch, E., "Light Emission in Photonic Crystal Micro-Cavities", Confined Electrons and Photons: New Physics and Applications, Proceedings of the International School of Materials Science and Technology at the Ettore Majorana Centre, Erice, Sicily, Italy, July 1993. (Plenum, New York, 1994).

Cheng, C.C., Arbet-Engels, V., Scherer, A., Yablonovitch, E., "Nanofabricated Three Dimensional Photonic Crystals Operating at Optical Wavelengths," Physica Scripta, Vol. T68, pp. 17-20, 1996.

Sievenpiper, D.F., Sickmiller, M.E., Yablonovitch, E. "3D Wire Mesh Photonic Crystals," Physical Review Letters, Vol. 76(14), pp. 2480-2483, April 1996.

Sievenpiper, D.F., Sickmiller, M.E., Yablonovitch, E. "3-D Metallic Photonic Bandgap Structures," CLEO '96 Technical Digest, Vol. 9, p. 387, Anaheim, CA, June 2-7, 1996.

Yablonovitch, E., Sievenpiper, D.F. "Knitting a Finer Net for Photons," Nature, Vol. 383, pp. 665-666, October 1996.

Cheng, C.C., Scherer, A., Arbet-Engels, V., Yablonovitch, E. "3-D Photonic Crystals Operating at Optical Wavelengths," Quantum Electronics and Laser Science Conference (QELS), Berlin, Germany, June 2-7, 1996 (Invited Paper)

Scherer, A., Yablonovitch, E. "Photonic Band Gap Structure," 23rd International Conference on the Physics of Semiconductors, Berlin, Germany, July 16-21, 1996. (Invited Paper)

Cheng, C.C., Scherer, A., Arbet-Engels, V., Yablonovitch, E. "Lithographic Band Gap Tuning in Photonic Band Gap Crystals," J. Vac. Sci. Technol., Vol. 14(6), pp. 4110-4114, November/December, 1996.

Scherer, A., O'Brien, J., Cheng, C.C., Painter, O., Lee, R., Yablonovitch, E., Yariv, A. "Microfabrication of Photonic Crystal Mirrors for Optoelectronic Devices," OSA Quantum Optoelectronics Technical Digest, pp. 38-39, Incline Village, Nevada, March 19-21, 1997.

Yang, H.-Y. D., Alexopoulos, N.G., Yablonovitch, E. "Photonic Band-Gap Materials for High-Gain Printed Circuit Antennas," IEEE Transactions on Antennas and Propagation, Vol. 45(1), pp. 185-187, January 1997.

"2D Photonic Crystal Vertical Cavity Array for Nonlinear Optical Image Processing" by Sievenpiper etc. (submitted for publication).

4. Scientific Personnel

Dan Sievenpiper (qualified as Ph.d. candidate)
Vincent Arbet-Engels
Brian Hong
Mike Sickmiller (M. Sc.)

5. Reportable inventions

none

Section 2: Summary of the most important results
Preprint

2D Photonic Crystal Vertical Cavity Array for Nonlinear Optical Image Processing

by

D. F. Sievenpiper, C. F. Lam, E. Yablonovitch

Electrical Engineering Department

University of California, Los Angeles

Los Angeles, CA 90095-1594

ABSTRACT

We have investigated the electromagnetic properties of a two dimensional photonic crystal array of vertical cavities for use in nonlinear optical image processing. We have determined the two dimensional photonic band structure of the array, and we discuss how it is influenced by the degree of interaction between cavities. We have studied the properties of defects in the 2-D lattice, and have shown that neighboring cavities will interact through their overlapping wave functions. This interaction can be used to produce nearest neighbor nonlinear Boolean functions such as AND, OR, and XOR which are useful for optical image processing. We demonstrate the use of 2-D photonic band gap structures for image processing by removing noise from a sample image, employing a nearest neighbor AND function.

Most optical image processing systems use linear elements such as lenses, gratings, and masks to perform transformations on images. These can be used to carry out many important functions such as the Fourier transform of an image, the correlation of two images, various types of spatial filtering, and other linear operations [1]. Since these devices operate on an entire image at once, they exploit the inherently parallel nature of optical image processing systems. However, many operations require nonlinear functions which cannot be achieved without a nonlinear device [2]. Such operations are often accomplished with a digital computer, in which the nonlinear elements are transistors. Unfortunately, this requires the image to be processed pixel by pixel, and lacks the speed and parallelism of an optical image processing system.

We have found that a two-dimensional photonic crystal [3-8] array of vertical cavities can be used to implement several nonlinear functions which are useful for optical image processing. The cavities interact with each other through their overlapping wave functions, resulting in coupling between neighbors. To define an image on the array, some of the cavities are altered, causing a shift in their resonant frequency. As a result of inter-cavity coupling however, the magnitude of the frequency shift will depend not only on the state of the cavity, but also the states of its neighbors. This effect is used to create nonlinear functions between neighboring cavities including AND, OR, and XOR (exclusive-OR). We have applied this idea to demonstrate a noise removal process on a sample image using a nearest neighbor AND function.

Our experiments are performed in the microwave regime for simplicity, but the results may be extended to optical wavelengths by scaling the dimensions of the structure. The cavities consist of alternating layers of acrylic and polystyrene foam. The

acrylic layers have an index of refraction of 1.6, and the polystyrene foam has an index of refraction roughly equal to unity. They are cut to a thickness of 0.32cm and 0.52cm respectively, so that the thickness of each layer corresponds to one quarter of a wavelength at a frequency of 14.5GHz. Ten periods of alternate layers are stacked to form a Bragg mirror. An additional quarter wavelength of foam is then inserted into the center of the stack to form a resonant cavity.

Our array is made up of a triangular lattice of these vertical cavities. We chose a triangular lattice since that is the most intuitively natural geometry in two dimensions, however the square lattice of vertical cavities [6] also produces interesting results. Each cavity measures 3.81cm from side to side, and is hexagonally shaped to perfectly fill two-dimensional space. Foam spacers with a width of 0.3cm are used to laterally separate the cavities. The entire array is held between two acrylic support plates measuring 2.5cm thick. Roughly forty cavities make up our sample, a section of which is shown in Fig. 1.

Because of the lateral periodicity, the array of cavities forms a two-dimensional photonic crystal. In order to determine the nature of the interaction between the cavities, we investigated the two-dimensional photonic band structure of our lattice. Measurements were performed using a Hewlett-Packard 8720 network analyzer, with horn antennas for transmitting and receiving. The structure was placed between the transmitting and receiving antennas, and rotated with respect to the incoming waves. The waves have a large wave vector component, $k_{\perp}$, which is perpendicular to the plane of the lattice as indicated by the arrows in Fig. 1. The rotation produces a small parallel component, $k_{\parallel}$ which lies within the plane of the array. We constructed the two-dimensional photonic dispersion relation by measuring the resonant frequency of the

cavities as a function of $k_{||}$. In most work on 2D photonic crystals, the waves travel entirely in the plane of the 2D lattice. Here, the wave vectors are primarily directed perpendicular to lattice, with only a small parallel component, as in the work done by Russel, et. al. on optical fiber photonic crystals [7].

The evolution of the band structure can be seen by measuring the dispersion relation with and without the foam spacers between the cavities. Without the spacers, the cavities are tightly packed together. The structure exhibits a $1/\cos(\theta)$ relationship between the resonant frequency and $k_{||}$, as shown in the curved solid line in Fig. 2. This may be regarded as the empty lattice scenario. When small foam spacers are included between the cavities, the frequencies are the same except that gaps appear near the edges of the Brillouin zone. The gaps, centered around 15GHz, separate the dispersion curve into energy bands, as indicated by the solid and empty points in Fig. 2. The width of the bands is a measure of the degree of interaction between the cavities, analogous to the overlap integral [9] in an atomic crystal lattice. With 0.3cm spaces between cavities, the lowest band has a width of about 300MHz.

In a triangular lattice, the electromagnetic interaction between the cavities is particularly complicated. For example, a triangular lattice exhibits frustration [10], which is absent in a square lattice. Frustration occurs when geometry forbids each lattice point from being polarized opposite to all of its neighbors at the same time. Nonetheless, the nearly-free-photon model can be used to determine the energy levels and corresponding electric fields at certain symmetry points in the Brillouin zone. At the L-point for instance, on the Brillouin zone inset in Fig. 2, the incident wave is coupled to an opposing wave which is reflected from the nearest point in the inverse lattice. The

resulting standing waves form two energy levels corresponding to an air band and a dielectric band [5]. In real space, the dielectric band includes states in which the peak electric field occurs in the center of the cavities, while in the air band the cavities sit on the nodes of the standing waves. Both s- and p-polarization states are possible, so each of these levels is doubly degenerate, and there is no mixing between polarization states.

At the H-point, the situation is more interesting. In addition to the incident wave, there are two nearby points in the reciprocal lattice which contribute reflected waves. There are also two polarization states, for a total of six interacting waves. Again, the nearly-free-photon model can determine the relative amount of coupling between each wave. The various coupling constants form the basis of an eigenvalue problem which yields the energy levels and related electric field patterns. There are four energy levels at the H-point, and the middle two are each doubly degenerate. The lowest is the swirl pattern shown in Fig. 3a, which is entirely s-like. The highest is the p-like hedgehog pattern of Fig. 3b. The four remaining modes associated with the two middle energy levels have a mixture of both s and p characteristics. Experimentally the mixed nature of these states is confirmed by the observation of finite transmission peaks at the H-point which are seen when the transmitting and receiving antennas are cross-polarized. Not all energy levels at the H-point are observed, but this may be because some modes do not couple well to free space.

Until now, we have described the properties of a homogeneous array in which all the cavities are identical. In order to perform useful functions however, we must introduce "defects" into the lattice, making some of the cavities different. We now describe the properties of such "defects" and their relation to the band structure analysis

given earlier. A defect is created by altering the resonant frequency of one of the cavities. We do this by inserting an additional 0.16cm of acrylic into the center of the cavity, and removing an equal amount of foam to keep the overall layer spacing the same. This raises the effective index of refraction of the cavity, and therefore lowers its resonant frequency. The frequency shift is sensitive to the exact location of the additional layer, since the mode intensity varies along the length of the cavity. We place the additional layer of acrylic near the center of the cavity for maximum frequency shift. For the following experiments, we also remove the foam spacers from between the cavities to maximize the degree of interaction.

If one cavity is altered, and the rest of the array is left unchanged, that cavity will experience a frequency shift of about 750MHz, indicated in Fig. 2 by a solid horizontal bar. The length of the bar is meant to show that the localized state takes up a large area of k-space. Since the frequency shift is much larger than the width of the lowest energy band, we can conclude that the state is well localized to the altered cavity. If two neighboring cavities are altered however, the pair will experience a greater frequency shift, about 850MHz, indicated in Fig. 2 by the slightly lower horizontal bar. Thus, two altered cavities next to each other will have a different resonant frequency than either one would have by itself. If all of the cavities in the structure are altered, the resonant frequency of the array shifts downward by 1.1GHz. In this case the entire band structure is shifted downward, indicated by the lower set of curved solid lines in Fig. 2.

We have found that the resonant frequency of a particular cavity depends on its surroundings. This is because the mode of each cavity extends slightly into adjacent cavities, resulting in a coupling between nearest neighbors. In general, if two identical

resonators are allowed to interact, they will generate two new frequencies, one higher and one lower, centered around the original frequency of the resonators. This effect is seen in many examples, such as the bonding and anti-bonding modes of diatomic molecules, or in metallic photonic band gap structures with two interacting defects [8]. In the case of coupled vertical cavities, the interaction generates a low frequency symmetric mode and a higher frequency antisymmetric mode. We only detect the symmetric mode however, because we are illuminating the structure at normal incidence. Thus, the interaction manifests itself as a downward frequency shift, causing two adjacent altered cavities to resonate at a lower frequency than one isolated altered cavity.

This interaction between neighboring cavities can be put to use to perform several important nonlinear image processing functions. If a single isolated cavity is altered, it will resonate at a certain frequency, but if one of its neighbors is also altered, both cavities will resonate at a slightly lower frequency due to their interaction. If we measure the transmission at this lower frequency, we obtain the AND function between the two cavities. Both neighboring cavities must be altered in order to detect transmission at the proper frequency. This could be accomplished with a narrow-band filter which selects for the two-cavity resonance. We can also produce the XOR function by using a different filter with a pass band at the single-cavity resonance. In this way, we only detect transmission if one isolated cavity is altered, but none of its neighbors. Furthermore, if we use a filter with a wide pass band which includes both frequencies, we generate the OR function. We would then detect transmission either if an isolated cavity is altered, or if two neighboring cavities are altered. These functions are slightly different from the usual Boolean functions of the same names because they are carried out in a two-

dimensional lattice. Each operation is actually a function of the state of each cavity and all six of its nearest neighbors.

The results described above can be used to produce important optical image processing functions. We demonstrate this by using the nearest neighbor AND function to remove noise from a sample image. Fig. 4a shows an image of the number "7" with some pepper noise added in the form of two erroneous black pixels. Pepper noise appears as black spots on a white background, as opposed to salt noise, which is white spots on a black background [11]. The black shading in fig. 4a denotes which pixels have had their resonant frequencies lowered in our vertical cavity array. We measured the transmission spectrum of each cavity by placing the receiving horn against the acrylic support plate on the front of our structure. Fig. 4b shows the results of transmission measurements at the frequency corresponding to altered pixels with several nearest neighbors altered. This criterion applies to most of the pixels in the "7" but not the noise pixels because they are isolated. Black shading is used in fig. 4b to denote the pixels with transmission greater than -12dB within the selected frequency range. Note that the single isolated altered cavities do not appear because they resonate at a slightly higher frequency. We have effectively removed the pepper noise from the image using the electromagnetic interaction between the cavities. Fig. 4c shows the transmission at the frequency of the single-cavity resonance. The noise pixels appear in this figure, as expected, because they are isolated cavities. The pixels at the ends of the number "7" also showed a small amount of transmission at both frequencies. The end pixels have only one nearest neighbor which is altered, so their transmission spectrum appears slightly different from the other pixels in the image.

We also attempted use this technique to remove salt noise, or white spots on a black background. We did this using an entire array of altered cavities, and several isolated unaltered cavities.. The band structure of this array is the lower set of solid curves in Fig. 2, which is shifted downward because the bulk of the array has been altered with an extra acrylic layer. The single unaltered cavity, with its higher resonant frequency, attempts to create a defect state above the bottom of the energy band. However, states already exist at this higher frequency, since the energy band of the lattice extends upward. These higher states are waves with large lateral wave vectors traveling in the bulk of the lattice. As a result, there is strong coupling between the mode of the isolated, unaltered cavity and the bulk. The mode therefore has a very low Q factor, and is not detected in transmission measurements. This represents an interesting asymmetry between the two types of cavities.

In conclusion, we have presented the two-dimensional band structure of a triangular array of vertical cavities. We have introduced defects into the lattice in the form of cavities which have been altered by a slight increase in dielectric constant, to produce a downward shift in resonant frequency. We have shown that these defects produce localized states below the energy band of the lattice. Furthermore, we have found that these altered cavities interact with each other to produce nonlinear Boolean logic functions. Specifically, nearest neighbor AND, OR, and XOR functions have been described. Finally, we have demonstrated an important image processing transformation by removing pepper noise from a sample image. We have also found an interesting asymmetry between low frequency altered cavities and higher frequency unaltered cavities due to the relative location of the energy band and the defect state involved. The

vertical cavity array has been shown to be a useful image processing element which can produce nonlinear logic functions with the inherent speed and parallelism of optical image processing systems.

This research was supported by the U.S. Army Research Office, contract number DAAH04-93-G-0227; the National Science Foundation, contract number ECS-9307088; and the U.S. Air Force/Office of Scientific Research, contract number F49620-95-0534.

References:

1. J. W. Goodman, Introduction to Fourier Optics, McGraw-Hill, New York, 1986
2. S. H. Lee, ed., Optical Information Processing Fundamentals, Springer-Verlag, New York, 1981
3. E. Yablonovitch, Phys. Rev. Lett. 58, 2059 (1987)
4. S. John, Phys. Rev. Lett. 58, 2406 (1987)
5. J. D. Joanopolous, R. D. Meade, and Joshua N. Winn, Photonic Crystals, Princeton University Press, Princeton, 1995
6. P. L. Gourley, M. E. Warren, G. A. Vawter, T. M. Brennan, and B. E. Hammons, Appl. Phys. Lett., 60, 2714 (1992)
7. T. A. Birks, P. J. Roberts, P. St. J. Russel, D. M. Atkin, et. al., Elec. Lett. 31, 1941 (1995)
8. D. F. Sievenpiper, M. E. Sickmiller, and E. Yablonovitch, Phys. Rev. Lett. 76, 2480 (1996)
9. N. W. Ashcroft, N. D. Mermin, Solid State Physics, Saunders College Publishing, New York, 1976
10. P. W. Anderson, Journal of the Less Common Metals, 63, 291 (1978)
11. T.-H. Chao, "Dyanmically Reconfigurable Optical Morphological Processor and its application," in Optical Information Processing Systems and Architectures 4, B. Javidi, ed., Proc. SPIE 1772, 21 (1992)

Figure Captions

1) Diagram of single vertical cavity and a section of the array. Arrows indicate the large perpendicular component of the wave vector and the small parallel component in the plane of the array.

2) Photonic band structure of the vertical cavity array. Solid curves represent the structure without spaces between the cavities, as in the empty lattice model. Filled and empty data points show measurements taken for s- and p- polarization, when the cavities are spaced by 0.3cm, producing gaps. Solid horizontal bars indicate the energy levels of a single frequency shifted cavity and a pair of altered cavities within the array. The Brillouin zone is included for reference.

3) (a) The highest energy level at the H-point on the top face of the Brilloiun zone is composed entirely of p-waves, and the electric field produces a hedgehog pattern. (b) The lowest energy level is composed entirely of s-waves, and the electric fields produce a swirl pattern.

4) (a) The original image of a number "7" with pepper noise. Black shading indicates which cavities have been altered with an extra layer of acrylic. (b) The nearest neighbor AND function removes the pepper noise, leaving the image of the number "7" intact. Black pixels are those with a transmission of more than -12dB within a narrow frequency range. (c) Measuring at a higher frequency detects the single cavity resonance associated with pepper noise. The end points of the "7" also have some transmission at this frequency.

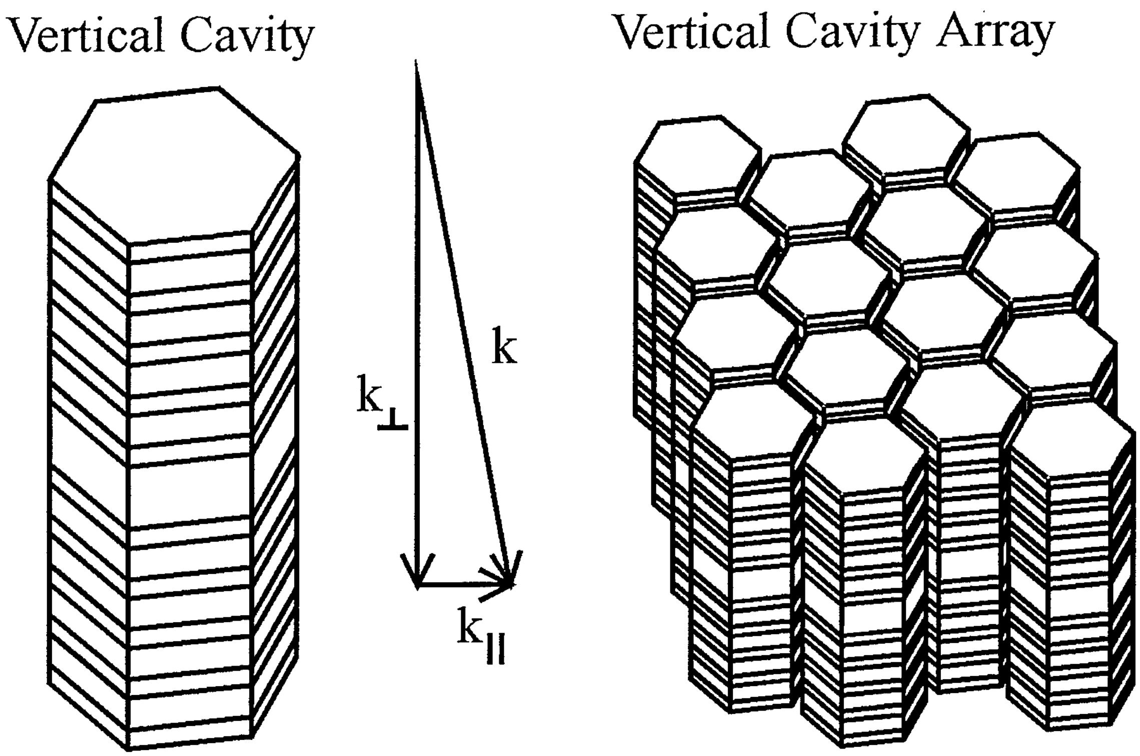

fig 1

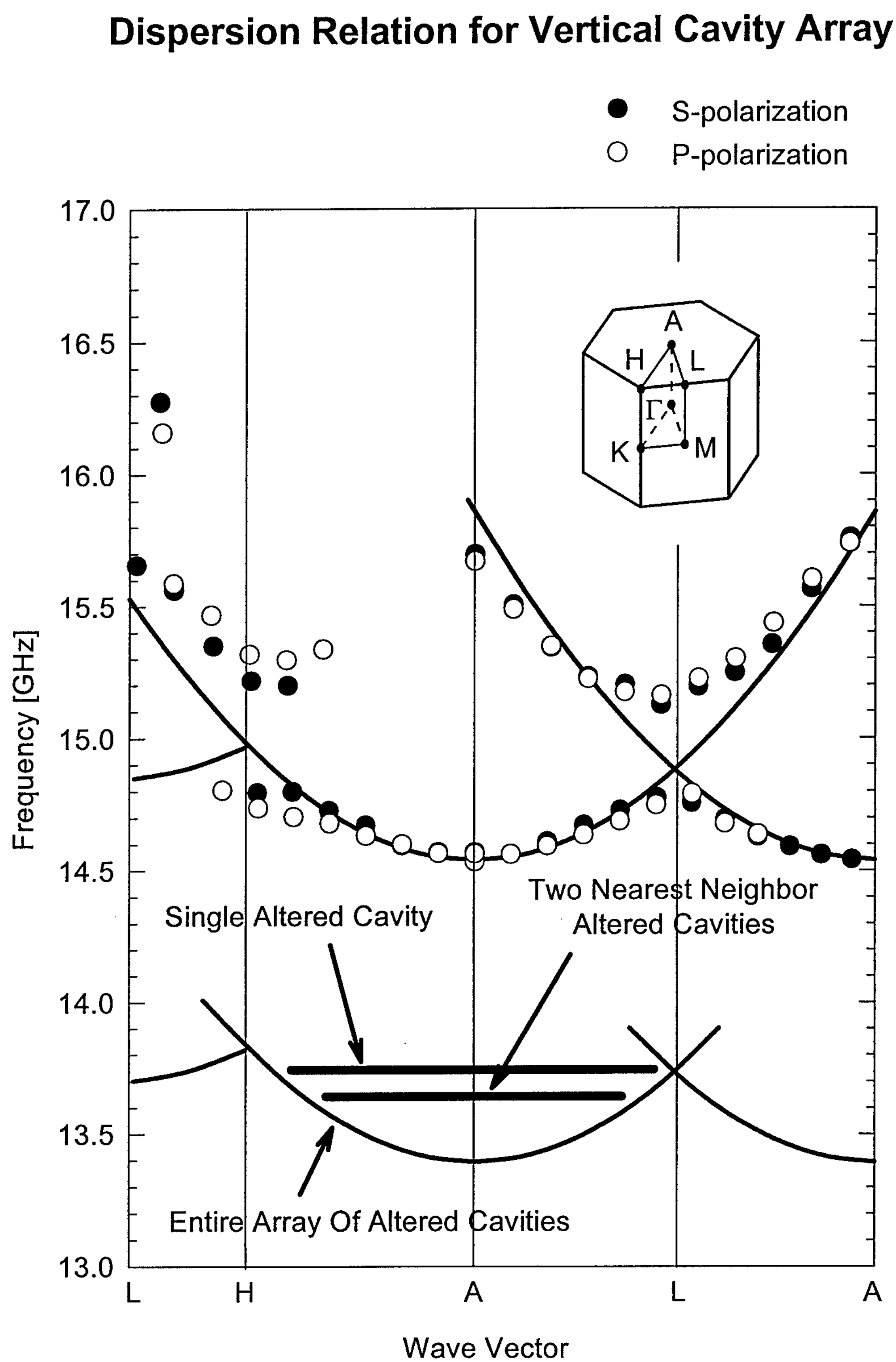

Dispersion Relation for Vertical Cavity Array
S-polarization
P-polarization
17.0
16.5
16.0
15.5
15.0
14.5
14.0
13.5
13.0
Frequency [GHz]
A
H
L
Γ
K
M
Two Nearest Neighbor
Altered Cavities
Single Altered Cavity
Entire Array Of Altered Cavities
L
H
A
L
A
Wave Vector

fig 2

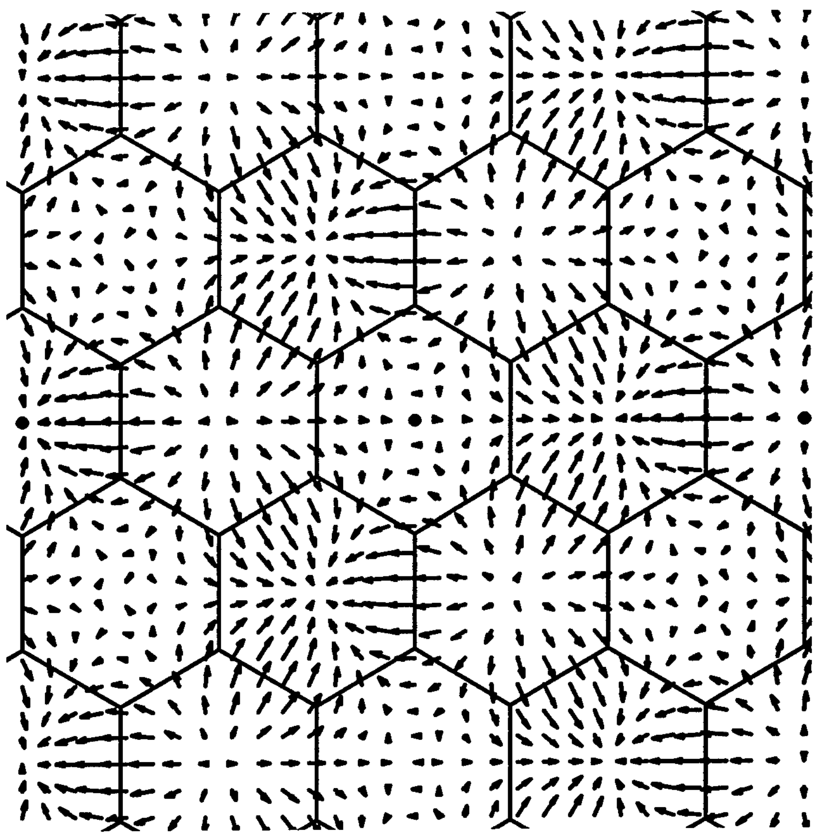

fig 3a

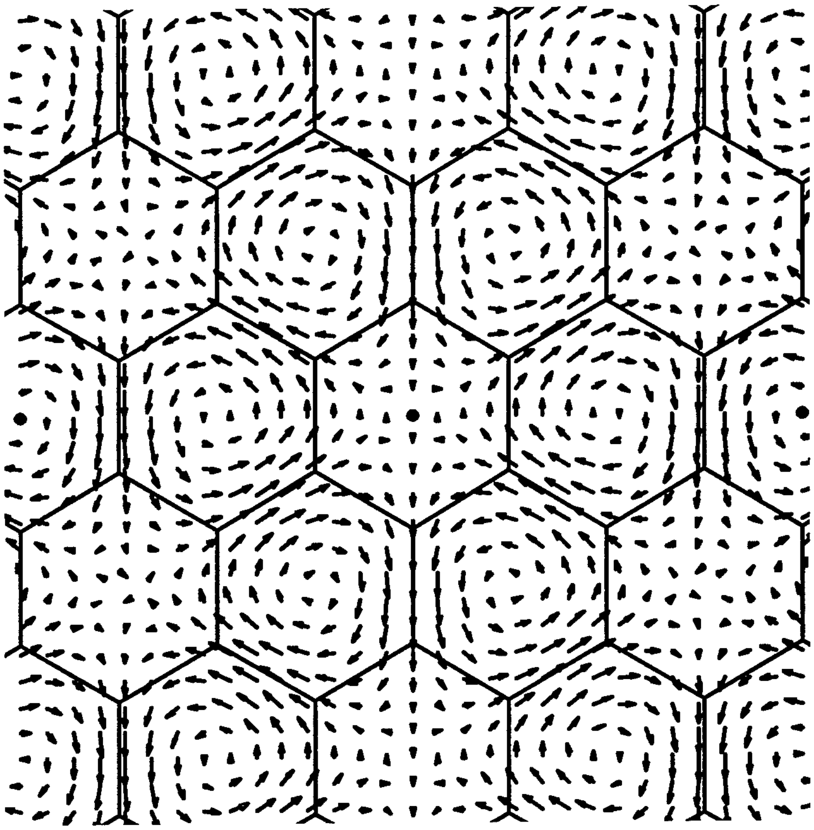

fig 3b

Original Image with Noise

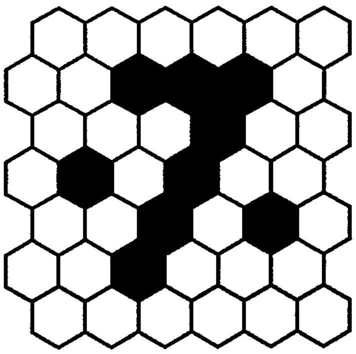

Nearest Neighbor "AND"
Function Removes Noise

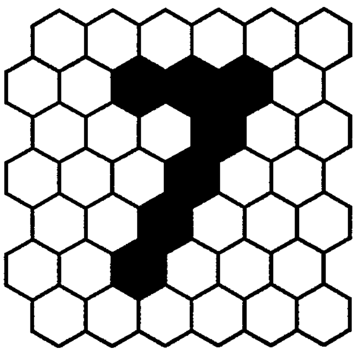

Image Illuminated at
Single-Cavity Resonance

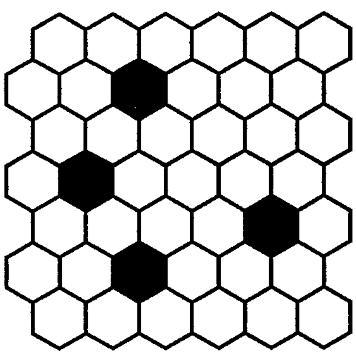

fig 4